The International Journal of Biochemistry & Cell Biology 76 (2016) 1–11

Contents lists available at ScienceDirect

The International Journal of Biochemistry & Cell Biology

journal homepage: www.elsevier.com/locate/biocel

PIWI-interacting RNA (piRNA) signatures in human cardiac progenitor cells

Serena Vella[a,b,*], Alessia Gallo[a,b], Antonio Lo Nigro[b], Daniele Galvagno[a,b], Giuseppe Maria Raffa[c], Michele Pilato[c], Pier Giulio Conaldi[a,b]

[a] Fondazione Ri.MED, Palermo, Italy
[b] Department of Laboratory Medicine and Advanced Biotechnologies, IRCCS- ISMETT (Istituto Mediterraneo per i Trapianti e Terapie ad Alta Specializzazione), Palermo, Italy
[c] Department for the Treatment and Study of Cardiothoracic Diseases and Cardiothoracic Transplantation, IRCCS- ISMETT (Istituto Mediterraneo per i Trapianti e Terapie ad Alta Specializzazione), Palermo, Italy

ARTICLE INFO

Article history:
Received 26 August 2015
Received in revised form 1 April 2016
Accepted 25 April 2016
Available online 27 April 2016

Keywords:
Cardiac progenitor cells
Cardiospheres
Cardiosphere-derived cells
piRNA

ABSTRACT

Cardiac progenitors, such as cardiospheres and cardiosphere-derived cells, represent an attractive cell source for cardiac regeneration. The PIWI-interacting RNAs, piRNAs, are an intriguing class of small non-coding RNAs, implicated in the regulation of epigenetic state, maintenance of genomic integrity and stem cell functions. Although non-coding RNAs are an exploiting field in cardiovascular research, the piRNA signatures of cardiac progenitors has not been evaluated yet.We profiled, through microarrays, 15,311 piRNAs expressed in cardiospheres, cardiosphere-derived cells and cardiac fibroblasts. Results showed a set of differentially expressed piRNAs (fold change ≥ 2, $p < 0.01$): 641 piRNAs were upregulated and 1,301 downregulated in the cardiospheres compared to cardiosphere-derived cells, while 255 and 708 piRNAs resulted up- and down-regulated, respectively, if compared to cardiac fibroblasts. We also identified 181 piRNAs that are overexpressed and 129 are downregulated in cardiosphere-derived cells respect to cardiac fibroblasts.Bioinformatics analysis showed that the deregulated piRNAs were mainly distributed on few chromosomes, suggesting that piRNAs are organized in discrete genomic clusters.Furthermore, the bioinformatics search showed that the most upregulated piRNAs target transposons, especially belonged to LINE-1 class, as validated by qRT-PCR. This reduction is also associated to an activation of AKT signaling, which is beneficial for cardiac regeneration.The present study is the first to show a highly consistent piRNA expression pattern for human cardiac progenitors, likely responsible of their different regenerative power. Moreover, this piRNome analysis may provide new methods for characterize cardiac progenitors and may shed new light on the understanding the complex molecular mechanisms of cardiac regeneration.

1. Introduction

Cardiovascular diseases are the leading cause of mortality and morbidity in the developed world (Nichols et al., 2014; Yeh et al., 2010), partly because mammals are not able to regenerate heart tissue (Aguirre et al., 2013). The presence of myocardial scarring predisposes to unfavourable left ventricular remodelling and heart failure (Yeh et al., 2010). The final goal of regenerative medicine for myocardial infarction (MI) is to reduce the scar formation, rebuilding a healthy heart muscle. In the absence of curative treatments, innovative biotechnological approaches aim to induce cardiac regeneration in patients with MI or heart failure, by delivering nucleic acids, recombinant proteins, or cells. Interestingly, the discovery of cardiovascular progenitor cells (CPC) in adult hearts has provided candidates for cell therapy approach (Wu et al., 2008), with some preclinical evidence for efficacy in cardiac repair and functional improvement after MI through both direct and indirect mechanisms (Chimenti et al., 2010). Following MI, resident CPC migrate from the niches to the site of injury, proliferate and finally differentiate into functional cardiomyocytes. At the same

Abbreviations: MI, myocardial infarction; CPC, cardiac progenitor cells; CS, cardiospheres; CDC, cardiosphere-derived cells; ncRNA, non-coding RNA; piRNA, PIWI-interacting RNA; CF, cardiac fibroblasts; RT, retrotransposons.

* Corresponding author at: Fondazione Ri.MED, Department of Laboratory Medicine and Advanced Biotechnologies, IRCCS- ISMETT, via Tricomi 5, 90127 Palermo, Italy.
E-mail address: sevella@ismett.edu (Vella S.).

http://dx.doi.org/10.1016/j.biocel.2016.04.012

time, the paracrine secretion of growth factors, cytokines and regulating nucleic acids is strongly involved in CPC-induced beneficial effects (Barile et al., 2014). CPC derived from human atrial or ventricular biopsies as well as from murine hearts were primarily described by Messina et al. (2004) (Chimenti et al., 2010,2012). These progenitors can be maintained in suspension as undifferentiated self-adherent 3D-clusters, called "cardiospheres" (CS), or adapting them to adherent plates as cardiosphere-derived cells (CDC). Interestingly, CS mimic a stem cell niche-like microenvironment with a high proportion of c-KIT+ cells and upregulated expression of SOX2, NANOG, and adhesion/extracellular (ECM) matrix molecules (Li et al., 2010). Dissociation of CS into single cells and their expansion in monolayers (CDC) decrease the expression of ECM molecules (Li et al., 2010) and reduce the heterogeneity of the cell population ameliorating the reliability of the *in vitro* analysis. Remarkably, CDC have been recently used in a phase 1 clinical trial (CADUCEUS), showing good results in term of safety and some evidences of therapeutic cardiac regeneration (Makkar et al., 2012).

For decades it had been supposed that heart loses the ability to regenerate after birth. On the contrary, recent studies have demonstrated that the capacity of cardiac repair is not totally lost in adults, where endogenous regeneration, after cardiac injury, is persistent, even if at a very low rate (Zhang et al., 2015). However, the cellular and molecular mechanisms of cardiac regeneration remain still unclear. Recently it has been demonstrated that different classes of non-coding RNA (ncRNAs) are involved in the control of the gene regulatory programs in heart development and disease (Ounzain et al., 2013; Philippen et al., 2015; Wu et al., 2013).

Particularly, microRNAs have been described to play critical roles in cardiogenesis, regulation of cardiomyocyte proliferation and progress of cardiovascular diseases (Aguirre et al., 2014; Barile et al., 2014; Eulalio et al., 2012; Mathieu and Ruohola-Baker, 2013; Olson, 2014). PIWI-interacting RNAs (piRNA) are another family of ncRNAs whose importance in gene expression regulation is now increasingly evaluated (Iwasaki et al., 2015; Moyano and Stefani, 2015; Weick and Miska, 2014). piRNAs are ncRNAs of 26–32 nucleotides in length involved in the maintenance of genome integrity by modulating the expression of retrotransposons (Aravin et al., 2006, 2007; Brennecke et al., 2007; Girard et al., 2006; Moyano and Stefani, 2015; Watanabe et al., 2006), which span around 40% of the eukaryotic genome. PiRNAs are generated within unannotated heterochromatic regions of the genome, where transposons and repetitive elements are also present (Samji, 2009; Seto et al., 2007). Recent evidence demonstrate that piRNAs are also expressed in somatic cells (Sharma et al., 2001), including cardiomyocytes. Moreover, it has been recently highlighted that miRNAs and piRNAs influence AKT signaling pathway (Rajan et al., 2014), a crucial network in heart physiopathology (Lin et al., 2015). Thus, piRNAs could play a functional role in cardiomyocyte proliferation and regeneration, apart from that already proven for miRNAs (Pisano et al., 2015). Confirming an effect of piRNAs on AKT pathway could provide insights for innovative diagnostic and therapeutic approaches for cardiovascular diseases.

To investigate this hypothesis, the assessment of piRNome in different cardiac cell types is of primarily importance. Here, we compare the piRNome of CDC, CS and cardiac fibroblasts (CF) (i.e. cardiac cells with different regenerative potential), obtained from heart bioptic samples of adult patients undergoing cardiac surgery.

Our results demonstrate that their piRNA expression profiles significantly differ in the three cell types, identifying a specific signature. Moreover, the results of our experiments provide evidence that piRNome in cardiac progenitors is associated with inhibition of LINE-1 and activation of the prosurvival AKT signaling.

2. Materials and methods

2.1. Biopsy specimen processing and cell culture

CPC were obtained by right atrial specimens collected by patients undergoing cardiac surgery. The study was approved by the local Ethical Committee and all patients gave written informed consent to the collection. The investigation conforms to the declaration of Helsinki. For patient characteristics see Supplementary Table 1. CS and CDC were obtained and cultured from biopsies as previously described (Messina et al., 2004). Briefly, biopsies were cut into small fragments, removing connective tissue, then washed and enzymatically digested (0.025% Trypsin-EDTA, Sigma-Aldrich, Milan, Italy). The tissue fragments were cultured as "explants" on dishes coated with fibronectin (BD Biosciences, Franklin Lakes, NJ). After several days, a layer of stromal like cells arose from adherent explants over which small, round, phase-bright cells migrated. Once confluent, the cells surrounding the explants were harvested by enzymatic digestion (0.05% Trypsin-EDTA, Sigma-Aldrich). These cardiosphere-forming cells were seeded on poly-D-lysine- coated flasks (Sigma-Aldrich) in CS medium. Several days later, cells that remained adherent to the poly-D-lysine-coated dishes were discarded, whereas detached cardiospheres (CS) were plated on fibronectin coated dishes and expanded as monolayers. CDC were subsequently passaged in CS, for a maximum of 5 times. CDC were cultured in IMDM (Iscove's Modified Dulbecco's Medium, Sigma-Aldrich) supplemented with 100 Units/ml penicillin G, 100 μg/ml streptomycin, 2 mmol/L L-glutamine (Sigma-Aldrich) and 20% FCS (Lonza, Basel, Switzerland). The CS medium was 35% IMDM/65% DMEM:HAM-F12 (Sigma-Aldrich) with 100 Units/ml penicillin G, 100 μg/ml streptomycin, 2 mmol/L L-glutamine (Sigma-Aldrich), 3.5% FCS, 4% B27 (Gibco, Milan, Italy), 20 ng/ml bFGF (basic Fibroblast Growth Factor, PeproTech, London, UK), 10 ng/ml EGF (Epidermal Growth Factor, PeproTech), 40 nmol/L Cardiotrophin-1 (PeproTech) and 40 nmol/L thrombin (Sigma-Aldrich). From the same biopsies, CF were isolated and cultured in DMEM (Sigma-Aldrich), supplemented with L-glutamine, penicillin/streptomycin (Sigma-Aldrich) and 10% FCS (Lonza).

2.2. piRNA microarray analysis and statistics

Total RNA was extracted from each sample with the RNeasy kit (Qiagen, Valencia, CA) and then treated with DNase. RNA was labelled with Cy-3 and hybridized to Human HG19 piRNA Expression Oligo microarrays (ArrayStar, Rockville, MD) containing probes for 23,000 piRNAs selected from the National Center for Biotechnology Information (NCBI) database and mapped to the HG19 genome sequence using UCSC Blat. Then the arrays were scanned with Agilent DNA Microarray Scanner G2505C. A transcript was considered detectable if the signal intensity was higher than 3 times the maximal background signal and the spot coefficient of variation (SD/signal intensity) was <0.5. The expression data files obtained by the Agilent Feature Extraction Software were imported into GeneSpring GX software. The differentially expressed piRNAs were identified by fold-change screening with a threshold of 2 fold (Fig. 2A). Statistically significant differences between the groups were identified by GeneSpring statistics based on the *t* probability value method with high stringency (probability value of 0.001 to decrease the false-positives). Significant and differentially expressed piRNAs were identified through Volcano Plot filtering (Fig. 2B). Hierarchical clustering was performed using the Agilent GeneSpring GX software (version 12.1).

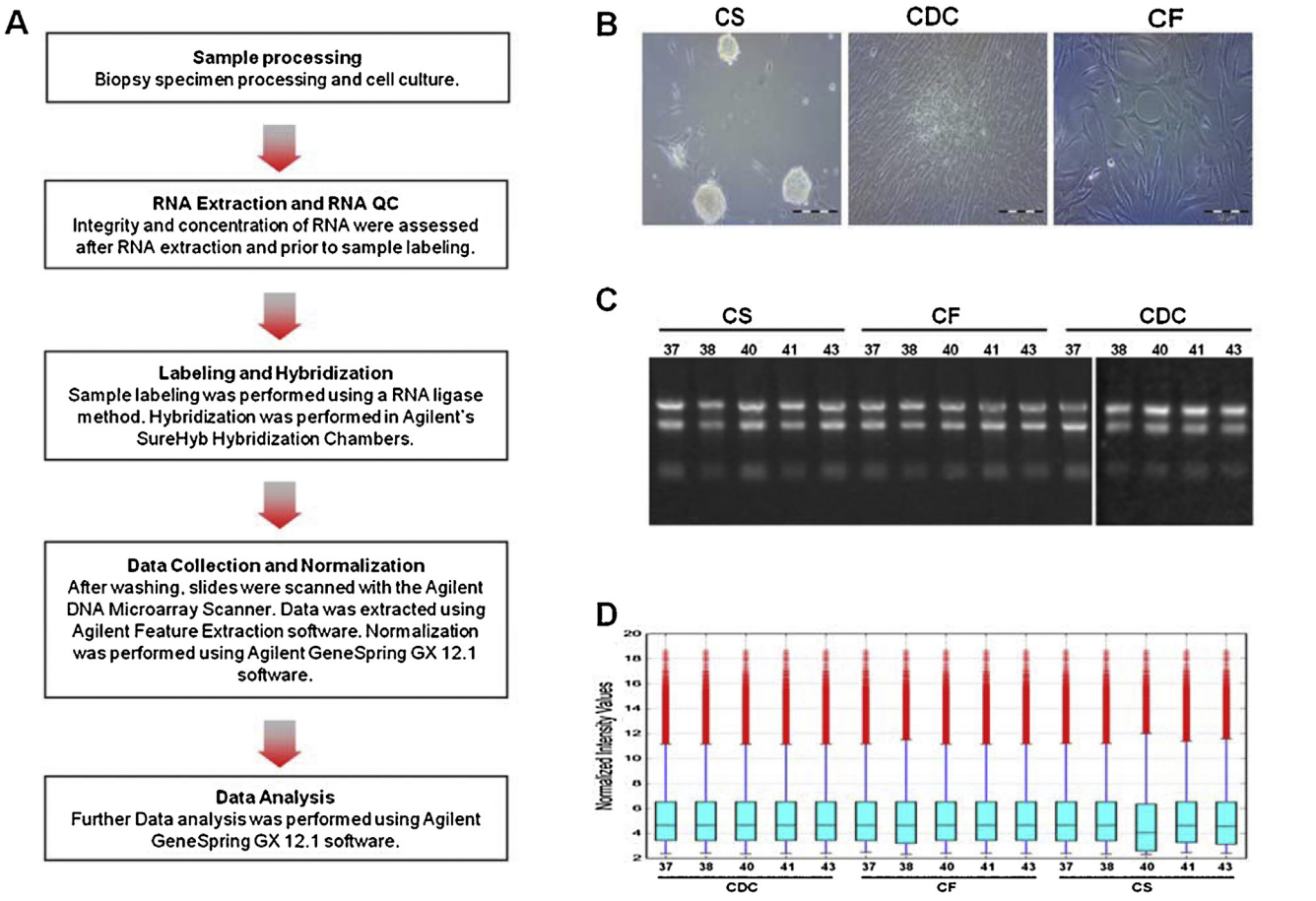

Fig. 1. piRNA profile in cardiospheres, cardiosphere-derived cells and cardiac fibroblasts.
A) Schematic representation of workflow of piRNA-screening in CS, CDC and CF. B) Representative photomicrographs of the three cell types. Magnification 10X. Scale bar: 50 μM. C) RNAs evaluation by denaturing agarose gel electrophoresis. D) piRNA profile comparison by box plot of log2 ratios distributions of piRNA datasets (n = 5 for each group).

2.3. Bioinformatics

To obtain a chromosome-wide piRNA distribution, the genomic locus for each piRNA was determined from piRNABank (Institute of Bioinformatics and Applied Biotechnology, Bangalore, India; http://pirnabank.ibab.ac.in). In addition, we analysed the targets of the upregulated piRNAs in CS, CDC and CF, using a modified version of miRanda in piRNABank. Each piRNA was searched for repeat sequence targets against the transposon database of the human chromosomes (NCBI Human Genome Build 36) across a representative 100,000 base stretch (position 1–100,000) with a mean free energy maximum of 20.0 kcal/mol and a very stringent score threshold of 140.

2.4. Real-Time RT-quantitative PCR (qRT-PCR)

Quantitative RT-PCR (qRT-PCR) was performed to validate the microarray results. Total RNA was isolated from CDC, CS and CF, using miRNeasy mini kit (Qiagen, Germany), according to the manufacturer's instructions.

2.4.1. Characterization of cell types

Reverse transcription was performed using the High-Capacity cDNA Reverse Transcription Kit (Life Technologies, Thermo Fisher Scientific, Waltham, MA, USA) according to the manufacturer's instructions to obtain cDNA. Gene expression was quantified by qRT-PCR using StepOnePlus Real-Time instrument (Applied Biosystems, Thermo Fisher Scientific) using TaqMan or Sybr Green methods. TaqMan gene assays (Life Technologies, Thermo Fisher Scientific) for DDR2 (Hs01025953_m1), CD90 (Hs00174816_m1), CD45 (Hs00365634_g1), CD31 (Hs00169777_m1), VIM (Hs00958113_g1), CD105 (Hs00923996_m1), cTNT (Hs00943911_m1), CX43 (Hs00748445_s1), SMA (Hs00426835_g1) and GAPDH (Hs02758991_g1) were used. The sequences of forward and reverse primers for Sybr Green method were: FLK1 Forward 5′-AGCCTTCAGATGCCACAGAC-3′ and Reverse 5′-ACAACCAGACGGACAGTGGT-3′; GATA4 Forward 5′-CTGTGCCCGTAGTGAGATGA-3′ and Reverse 5′-TCCAAACCAGAAAACGGAAG-3′; ISL1 Forward 5′-ATTTCCCTATGTGTTGGTTGCG-3′ and Reverse 5′-CGTTCTTGCTGAAGCCGATG-3′; GAPDH Forward 5′-ACCAGGAAATGAGCTTGACAAA-3′ and Reverse 5′-CGAGATCCCTCCAAAATCAA-3′. GAPDH was used as a reference gene for the relative quantification, assessed by $2^{-\Delta CT}$ calculation for each mRNA. The samples were run in duplicate and template-negative reactions served as controls.

2.4.2. Analysis of piRNAs

The TaqMan small RNA assays for piRNAs were custom designed (by Life Technologies, Thermo Fisher Scientific). DNase I–treated total RNA (1000 ng) were reverse-transcribed using the TaqMan MicroRNA Reverse Transcription Kit (Applied Biosystems, Thermo Fisher Scientific) following the manufacturer's protocol, with minor modifications as described (Lee et al., 2011). Expression of piRNAs was quantified by TaqMan RT-PCR using ABI PRISM 7900 Fast instrument (Applied Biosystems, Thermo Fisher Scientific) with

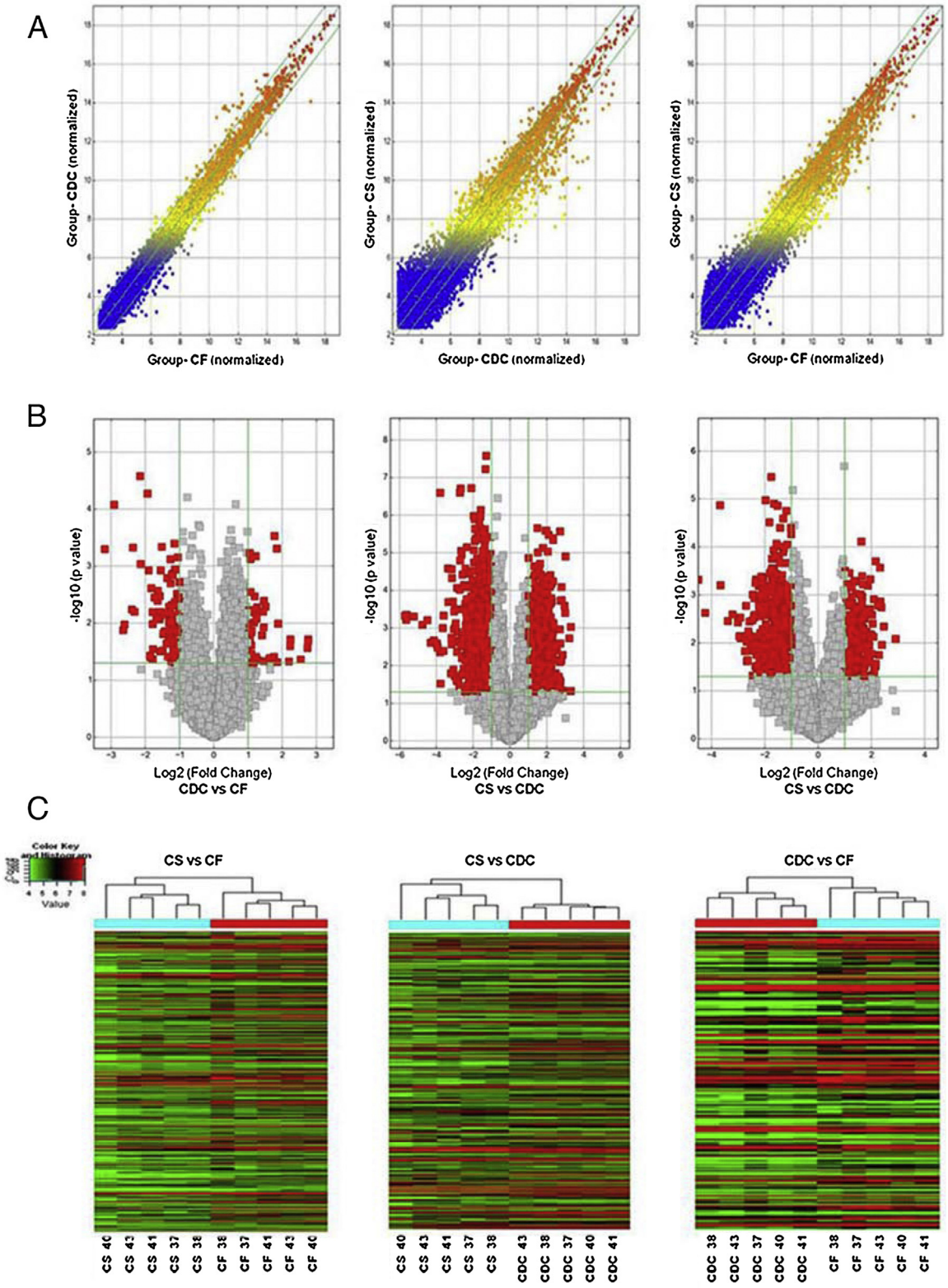

Fig. 2. Differentially expressed piRNAs in CS, CDC and CF.
A) Scatter plot of piRNA expression variation between the sample groups (n = 5 for each group). The values of X and Y axes are averaged normalized values in each group (log2 scaled). The green lines are fold-change lines (the default fold-change value given is 2). piRNAs above and below the green lines showed >2 fold increase or decrease, respectively, between pairs. B) Volcano plot of fold-change and corresponding p values for each piRNAs after comparison of the two sample groups (n = 5 for each group). C) Hierarchical clustering based on the expression levels of piRNAs in CS, CDC and CF (n = 5 for each group). The dendrogram shows the relationships among piRNA expression patterns: "red" indicates high relative expression, "blue" low relative expression. (For interpretation of the references to colour in this figure legend, the reader is referred to the web version of this article.)

assays designed by Life Technologies. U6 snRNA (001973) was used as a reference gene for the relative quantification, assessed by $2^{-\Delta\Delta CT}$ calculation for each piRNA. The samples were run in duplicate and template-negative reactions served as controls.

2.4.3. Analysis of L1 RNA transcripts

Reverse transcription was performed using the High-Capacity cDNA Reverse Transcription Kit (Life Technologies, Thermo Fisher Scientific, Waltham, MA, USA) according to the manufacturer's instructions to obtain cDNA. cDNAs were subsequently analyzed by qRT-PCR in a total volume of 20 μl mixture containing 1X TaqMan Universal MasterMix II (Life technologies, Thermo Fisher Scientific), 900 nM of each primer and 180 nM of TaqMan probe. For the quantification of L1 RNA transcripts, we used the primers and probes listed in Table 1, as already described (Coufal et al., 2009). The 5′-UTR primers/probe set is useful for the evaluation of the expression level of full-length transcripts, while the ORF2 oligonucleotides set provides an estimation of full-length transcripts plus other 5′ truncated LINEs. The samples were normalized according to the glyceraldehyde-3-phosphate dehydrogenase (GAPDH) mRNA (Hs99999905_m1, Life Technologies, Thermo Fisher Scientific) levels. The expression fold change was calculated by the $2^{-\Delta\Delta CT}$ method for each of the reference genes. All the samples were tested in triplicate and template-negative reactions served as controls.

2.5. Western blotting

Western blotting was carried out using whole-cell lysates. Briefly, total protein extraction was performed by homogenizing cells in RIPA lysis buffer containing protease inhibitors (Protease Inhibitor Cocktail Set II, 539132, Calbiochem, EMD Chemicals, Merck KGaA, Darmstadt, Germany) and phosphatase inhibitors (Roche, Germany). Lysates were incubated on ice for 30 min and centrifuged at 12,000*g* for 20 min at 4 °C. Supernatants were then quantified with Qubit® 3.0 Fluorometer (Life Technologies, Thermo Fisher Scientific). Proteins were separated on 4–12% SDS–PAGE gel (Invitrogen, Thermo Fisher Scientific) and transferred to nitrocellulose membranes (BioRAD, CA). Membranes were blocked for 1 h in 5% non-fat dried milk in Tris-buffered saline (TBS) and incubated overnight with antibodies against phospho-AKT (Ser473) (4060, Cell Signaling Technology, Denvers, CO, USA), or AKT (pan) (4691, Cell Signaling Technology), or phospho-GSK-3β (Ser9) (5558, Cell Signaling Technology), or GAPDH (8884, Cell Signaling Technology). The membranes were washed and incubated with anti-rabbit HRP conjugated secondary antibodies (7074, Cell Signaling Technology). All the antibodies were used in accordance with the manufacturer's instructions. The signal was captured using a ChemiDoc XRS (Bio-RAD). The level of expression of different proteins was evaluated by Image J analysis software (Wayne Rasband, NIH, Bethesda, MD; http://rsb.info.nih.gov/ij/). Total protein levels were normalized to GAPDH levels, and p-AKT protein level was normalized to AKT.

2.6. Data analysis and statistical analysis

Data processing and analysis were conducted using tools from RQ-manager (v1.2, Life Technologies, Thermo Fisher Scientific), DataAssist software (v 3.01, Life Technologies, Thermo Fisher Scientific), Microsoft Excel and Prism GraphPad V5.0d software (GraphPad Software, CA). Statistical significance of the observed differences among the various experimental groups was calculated using a two-tailed unpaired Student's *t*-test. P-values < 0.05 were considered to be statistically significant. In the figures, * and ** indicate statistical significance at $p < 0.05$ and 0.01, respectively.

3. Results

3.1. piRNAs are differentially expressed in cardiospheres, cardiosphere-derived cells and cardiac fibroblasts

To define the piRNA expression profile we isolated CS, CDC and CF from 5 biopsies (see Supplementary Table 1).

The primary cell cultures for each cell type showed a high homogeneity and a similar cell growth rate, and presented their typical cell morphology (Fig. 1B). For each sample, after RNA extraction, we verified RNA integrity and gDNA contamination (Fig. 1C).

To prove that the isolated cells belong to a particular cell type, we analyzed the mRNA level of several markers, by quantitative Real-Time RT-PCR (qRT-PCR) (Supplementary figure). CF, CDC and CS did not express CD45 and cTNT, indicating, respectively, the absence of hematological and cardiomyocytes contamination in the initial isolation. Islet-1, a cardiac transcription factor, was not detected in any group. Differently, CF, CDC and CS expressed the cardiac transcription factor GATA-4, a crucial cardiac transcription factor, indicative of their origin. Interestingly, in line with a previous study (Barile et al., 2013), CS expressed higher levels of GATA4.

As shown in supplementary figure, we confirmed in CF a higher expression of CD90, Vimentin, DDR2, SMA and CX43 than in CDC and CS. Moreover CF and CDC did not express CD31, while CD31 mRNAs was increased in 3D CS culture, as described (Li et al., 2010). CDC and CS expressed mesenchymal stem cell markers, such as CD90, CD105, and vimentin, but they had low levels of the fibroblast marker DDR2, excluding possible fibroblasts contamination. The CPC phenotype was also confirmed by the presence of mRNA for the gap junction protein connexin 43. FLK1, a vascular endothelial progenitor marker, used as a marker to characterize and isolate cardiac stem/progenitor cells, was overexpressed in CDC and CS, if compared to CF.

We determined the piRNA expression profile (piRNome) in the three cell types through microarray analysis. After quantile normalization, the distributions of the data sets appeared nearly the same (Fig. 1D). Microarray data of CS and CDC were compared to CF, which were used as control because of their limited regenerative potential (Smith et al., 2007).

Among the 23,000 piRNAs present in the dataset, we found 15,311 piRNAs expressed in all the three cell types. When comparing the piRNA expression levels between CS and CDC, we identified 2022 differentially expressed piRNAs (Fig. 2A, B; fold change ≥2.0, $p < 0.01$). Among those, 641 piRNAs were upregulated in CS compared to CDC (Supplementary Table 2), while 1381 piRNAs were downregulated (Supplementary Table 3).

Looking at the differentially expressed piRNAs between CS and CF, we found 255 upregulated and 780 downregulated piRNAs (fold change ≥2, $p < 0.01$; Fig. 2A, B) (Supplementary Tables 4 and 5, respectively).

Up to 181 piRNAs were differentially expressed in CDC when compared to CF (fold change ≥2, $p < 0.01$; Fig. 2A, B), among which 52 were upregulated, whereas 129 were downregulated (Supplementary Tables 6 and 7, respectively). Table 2 shows the partial results for the differentially expressed piRNAs.

We used hierarchical clustering analysis to arrange the samples into groups based on their expression levels. This analysis confirmed the relationships among samples and also showed systematic variations in the expression of piRNAs among the three cell types (Fig. 2C). Interestingly, there are some piRNAs that are overexpressed (DQ570332, DQ578426, DQ579582, DQ591185, DQ592096) or downexpressed (DQ570024, DQ570256, DQ570326, DQ570684, DQ570815, DQ570940, DQ571549, DQ571550, DQ571873, DQ578783, DQ579896, DQ580140, DQ582231, DQ582302, DQ582443, DQ582496, DQ583129, DQ584904, DQ587263, DQ587751, DQ590873, DQ591537, DQ591538,

Table 1
Primers and probes for L1 transcripts.

Target	Forward	Reverse	Probe
L1 5′ UTR #1	GAATGATTTTGACGAGCTGAGAGAA	GTCCTCCCGTAGCTCAGAGTAATT	AAGGCTTCAGACGATC
L1 5′ UTR #2	ACAGCTTTGAAGAGAGCAGTGGTT	AGTCTGCCCGTTCTCAGATCT	TCCCAGCACGCAGC
L1 ORF2 #1	TGCGGAGAAATAGGAACACTTTT	TGAGGAATCGCCACACTGACT	CTGTAAACTAGTTCAACCATT
L1 ORF2 #2	CAAACACCGCATATTCTCACTCA	CTTCCTGTGTCCATGTGATCTCA	AGGTGGGAATTGAAC

Table 2
No. of differentially expressed piRNAs in CS, CDC, and CF.

		Fold change 2–4	Fold change 4–7	Fold change > 7	Total
CS *vs* CDC	up	504	129	8	641
	down	1236	107	38	1381
CS *vs* CF	up	237	17	1	255
	down	694	74	12	780
CDC *vs* CF	up	45	7	0	52
	down	121	7	2	129

Table 3
Deregulated piRNAs (fold change ≥ 4, $p < 0.001$) chromosome location.

	upregulated piRNAs			downregulated piRNAs		
Chr no.	*CS vs CDC*	*CS vs CF*	*CDC vs CF*	*CS vs CDC*	*CS vs CF*	*CDC vs CF*
1	155	20	0	53	20	1
2	9	0	2	20	18	0
3	9	0	0	7	3	0
4	7	0	0	5	3	0
5	14	0	0	3	11	1
6	17	2	0	44	16	1
7	7	4	0	25	7	0
8	7	0	0	3	0	1
9	14	0	0	10	5	0
10	37	0	0	27	12	0
11	19	0	0	10	8	0
12	15	0	0	14	4	1
13	5	0	0	12	1	0
14	7	0	1	4	3	0
15	27	0	0	25	5	0
16	4	0	1	15	15	0
17	6	0	7	22	24	1
18	4	0	0	2	1	0
19	11	0	0	16	8	1
20	5	1	0	1	0	0
21	1	0	0	4	1	0
22	51	6	0	8	4	0
23	11	0	0	4	6	2
X	1	0	0	6	0	0
Y	1	0	0	0	0	0

X, Y = sex chromosomes.

DQ591926, DQ593270, DQ593595, DQ593707, DQ595111, DQ595878, DQ596280, DQ596850, DQ597074, DQ597396, DQ597397, DQ597403, DQ597941, DQ597968, DQ598180, DQ598181, DQ598182, DQ598204, DQ599003, DQ599147, DQ599786, DQ600950, DQ600951, DQ600952, DQ600961) in both CS *vs* CDC and in CS *vs* CF (fold change ≥4, $p < 0.01$; Fig. 3A and B), suggesting a functional role of these piRNAs in cardiospheres. DQ570326, DQ570339, DQ578783, DQ582302, DQ582496 were upregulated in CDC *vs* CF and downregulated in CS *vs* CDC, suggesting that they are expressed at high levels in CDC. Moreover, some piRNAs are downregulated in both CS *vs* CF and in CDC *vs* CF (DQ578075, DQ579896, DQ581624) (Fig. 3B), suggesting a role in cardiac fibroblasts where they are expressed at higher levels.

The analysis of the chromosomal locations of the deregulated piRNAs showed that they were distributed over all chromosomes but with higher density on some chromosomes (Table 3). Calculating the genomic density distribution of the upregulated piRNAs (number of piRNA loci per Mb of individual chromosome) in CS *vs* CDC and in CS *vs* CF, we found some hotspots of piRNA loci on chr. 22 (0.99 or 0.12, respectively, piRNA loci per Mb of chromosome) and chr. 1 (0.60 or 0.08, respectively), whereas the average on the other chromosomes was 0.15 or 0.01, respectively (Fig. 3C and D).

The upregulated piRNAs in CDC *vs* CF were mainly located on chr. 17 (0.11 piRNA loci per Mb of chromosome), in comparison with the average on the other chromosomes (0.05) (Fig. 3E). In CS *vs* CDC and in CS *vs* CF, the genomic density distribution of the downregulated piRNAs revealed that many piRNA loci were on chr. 17 (0.27 and 0.29, respectively), compared to the average of the other chromosomes (0.11 and 0.06, respectively) (Fig. 3C and D), meanwhile the downregulated piRNAs in CDC *vs* CF were distributed on chr. 19 (0.017), in respect to the average on the other chromosomes (0.003) (Fig. 3E).

These data are consistent with the idea that differentially expressed piRNAs could be located on euchromatic or heterochromatic regions, respectively, and map to discrete genomic clusters, as previously reported (O'Donnell and Boeke, 2007).

3.2. Validation of the microarray data using real-Time RT-PCR

To verify the microarray data, we randomly selected six differentially expressed piRNAs (DQ582302, DQ570326, DQ571873, DQ594975, DQ572313, and DQ586118) and validated their expression levels by qRT-PCR in three different CDC, CS and CF lines (n = 3 for each cell types).

The qRT-PCR results showed a consistently higher level of changes in piRNA expression than the microarray data, most likely because of the higher sensitivity of the assay and the employed normalization procedures, consistent with the results of Dallas et al. (Dallas et al., 2005) and Yuen et al. (Yuen et al., 2002).

In addition, the differences in the expression level were highlighted for those piRNA with Ct < 17 (DQ582302, DQ582496, DQ570326) or Ct ≥ 31 (DQ594975, DQ572313, DQ586118), as previously described (Morey et al., 2006).

In the first comparison (CDC *vs* CF), the microarray results were confirmed by qRT-PCR (DQ582302, DQ570326, DQ571873, DQ594975, and DQ572313), with the exception of DQ586118 (Fig. 4A). In the second group of comparison (CS *vs* CF), the qRT-PCR results for three piRNAs (DQ594975, DQ572313, DQ586118) were in agreement with the microarray data. However, for DQ582302, DQ570326, DQ571873, the two methods showed slightly different results (Fig. 4B). It must point out that, although the inherent issues about data normalization and different sensitivity as well as other possible factors influencing the correlation of the results of the two methods (Yuen et al., 2002; Chuaqui et al., 2002; Dallas et al., 2005; Morey et al., 2006; Ach et al., 2008), in our experimental setting, the pattern of expression modulation resulted to be fairly in agreement by both qRT-PCR and microarray analysis.

3.3. Upregulated piRNAs target all the classes of LINE RT spread over human genome, especially LINE-1

piRNA-machinery regulate transposable elements in several species (Siomi et al., 2011). Among the different classes of transposons, LTR and LINE represent their main targets (Ha et al., 2014).

Interestingly, it was demonstrated that piRNAs mediate suppression of LINE-1 retrotransposons (RT) (Di Giacomo et al., 2013)

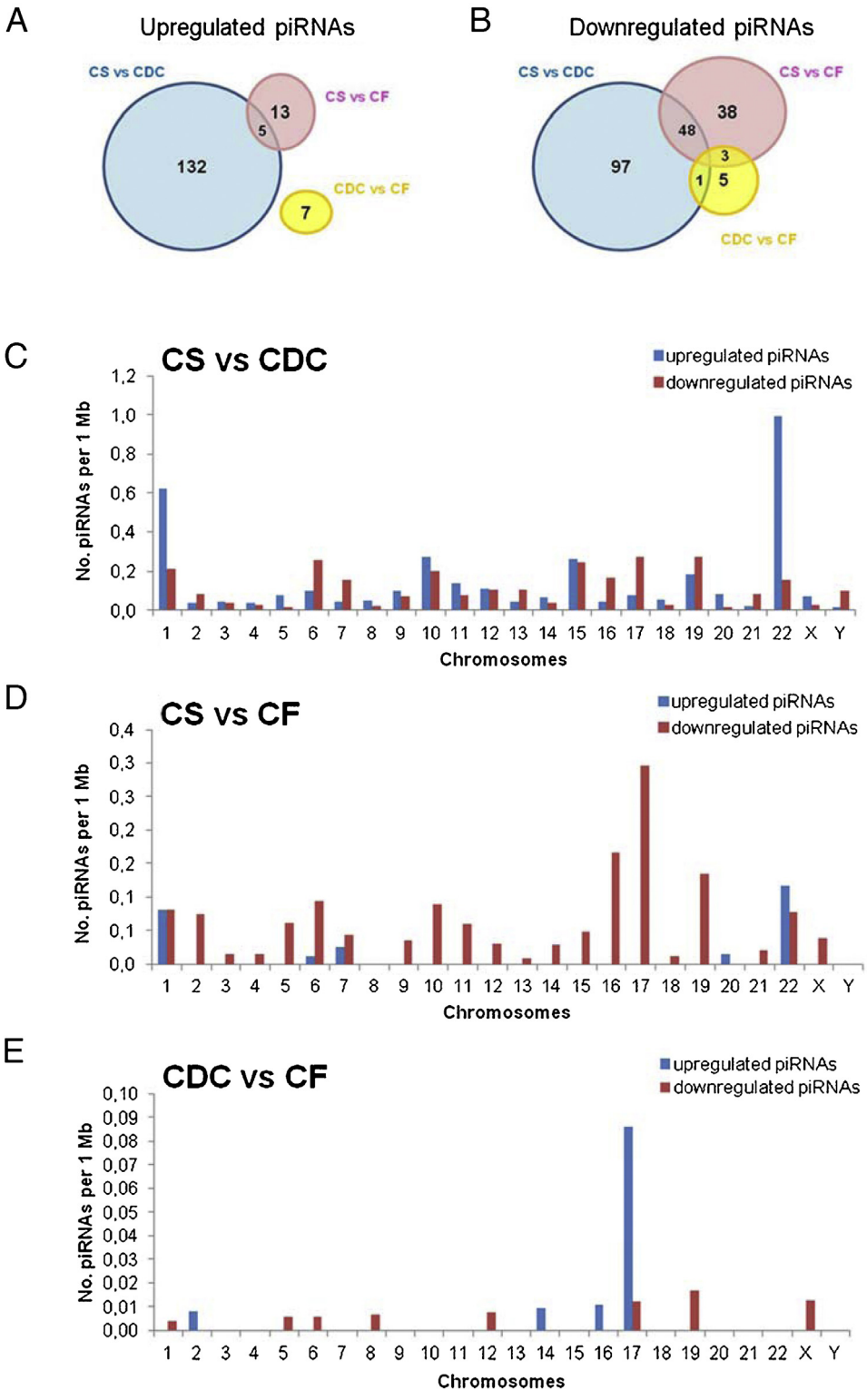

Fig. 3. Genomic distribution of the upregulated piRNAs.
Venn diagram showing the number of upregulated (A) or downregulated (B) piRNAs in the three comparison groups (n = 5 for each group). Densities of deregulated piRNAs on human chromosomes in CS *vs* CDC (C), in CS *vs* CF (D) and in CDC *vs* CF (E) expressed as number of piRNA loci per megabase of DNA of each chromosome.

and this inhibition was proven to be beneficial in decreasing the ischemic damage of the heart (Lucchinetti et al., 2006).

Based on this, we conducted a bioinformatics prediction of the LINE targets of each upregulated piRNAs searching in 100,000 base stretches (1–100,000 bases of each human chromosome). The number of targets of the upregulated piRNAs ranged from 20 to 483 with an average of 88.4 per 100,000 bases (Table 4).

Upregulated piRNAs targeted all the classes of LINE RT (LINE-1, LINE-2 and CR1) spread over human genome (Table 5), especially LINE-1. Thus, upregulation of piRNAs in CPC, mainly in CS, could

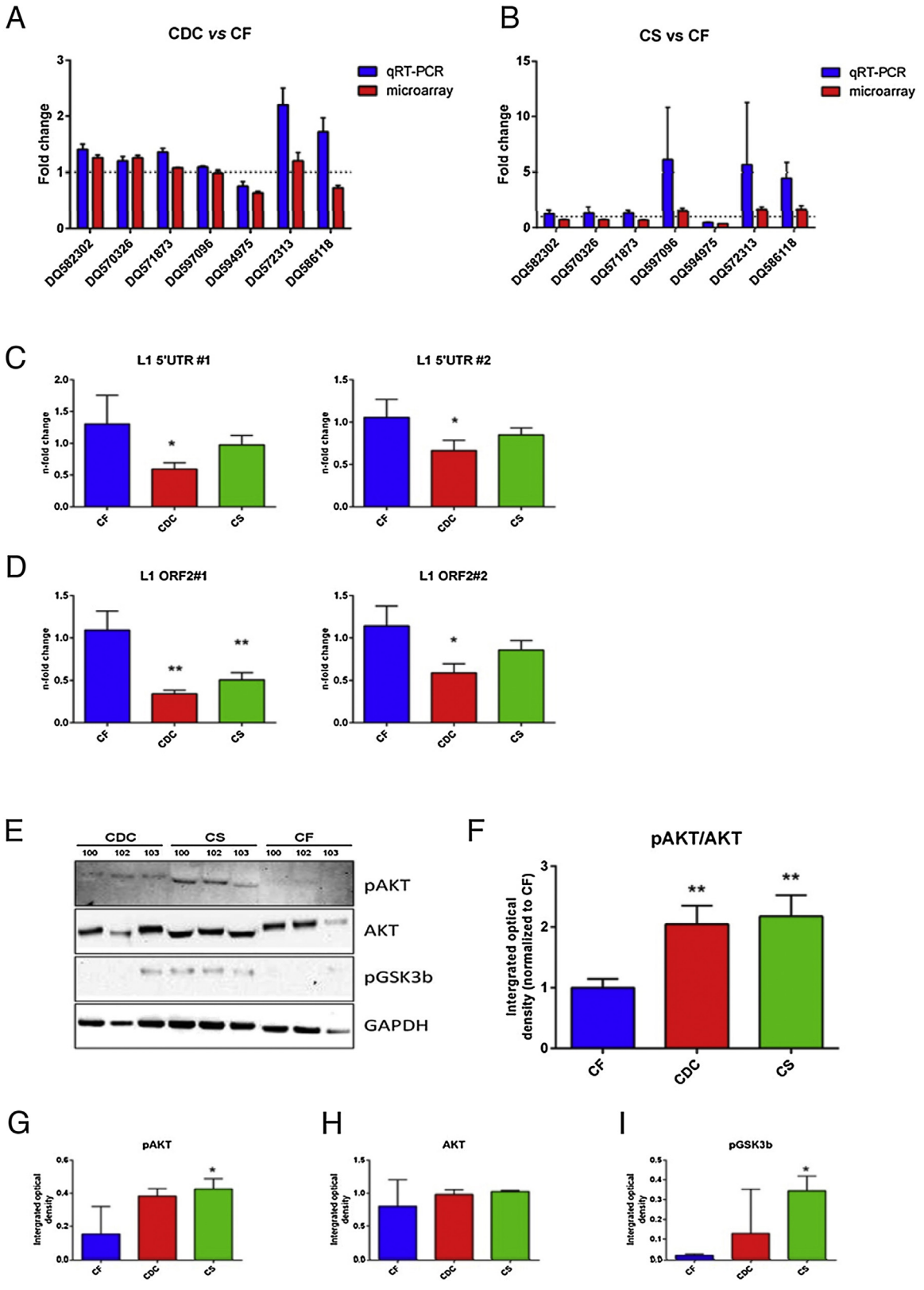

Fig. 4. piRNA deregulation is associated with L1 reduction and AKT signaling activation in cardiac progenitors.
Validation and comparison of microarray and qRT-PCR data. Values represent fold change in transcript copy number relative to control U6. Mean (± SD, n = 3) expression of the piRNAs DQ582302, DQ570326, DQ571873, DQ597096, DQ594975, DQ572313 and DQ586118, as measured by microarray and qRT-PCR in CDC *vs* CF (A) and in CS *vs* CF (B). Quantitative RT-PCR results for L1 RNA expression using the 5′ UTR #1 and #2 (C) or ORF2#1 and ORF2#2 (D) primer sets, analyzed in CDC, Cs and CF. The graphs show the fold change in L1 expression in CDC and CS comparing to CF. (E) Western Blot analysis of AKT, pAKT (S473), pGSK3β (S9) and GAPDH. (F) Densitometric analysis of the ratio pAKT/AKT showing statistically increased levels of the activated phosphor-AKT(S473) in CDC and CS, compared to the CF. Densitometric analysis of pAKT (G), AKT(H), pGSK3b (I), normalized to GAPDH. Densitometric analyses are expressed as means ± SD of three independent samples for each cell types. One star (*) indicates $p < 0.05$, while two stars (**) indicate $p < 0.001$, two-tailed Student's test.

Table 4
No. of targets of upregulated piRNAs (fold change ≥ 4, p < 0.001) distributed in bases 1–100,000 of the human chromosomes.

	Upregulated piRNAs in CS					Upregulated piRNAs in CDC					Upregulated piRNAs in CF		
Chr no.	DQ570332	DQ578426	DQ579582	DQ591185	DQ592096	DQ570326	DQ570339	DQ578783	DQ582302	DQ582496	DQ579896	DQ578075	DQ581624
1	5	10	4	8	20	0	0	2	0	7	1	5	0
2	5	16	4	0	24	0	0	3	0	5	3	7	0
3	6	3	4	3	5	0	0	0	0	0	2	5	0
4	0	0	5	0	38	0	0	9	0	4	0	5	0
5	4	2	1	4	14	0	0	2	0	1	0	2	0
6	15	0	4	12	0	0	0	6	0	4	0	5	0
7	9	3	2	2	8	0	0	2	0	1	1	6	0
8	14	7	0	3	71	0	0	5	0	1	0	10	0
9	14	3	4	10	0	0	0	5	0	6	1	1	0
10	6	11	3	7	33	0	0	4	0	2	2	5	0
11	12	12	2	7	29	0	0	4	0	1	0	6	0
12	3	8	3	12	21	0	0	4	0	3	2	5	0
13	0	0	0	0	0	0	0	0	0	0	0	0	0
14	5	0	0	0	0	0	0	0	0	0	0	0	0
15	0	0	0	0	0	0	0	0	0	0	0	0	0
16	1	2	0	3	56	0	0	0	0	0	1	1	0
17	2	5	2	2	35	0	0	2	0	1	1	5	0
18	7	11	5	7	31	0	0	4	0	1	2	6	0
19	10	11	4	8	36	0	0	3	0	6	0	7	0
20	10	20	4	14	58	0	0	5	0	6	4	12	0
21	0	0	0	0	0	0	0	0	0	0	0	0	0
22	0	0	0	0	0	0	0	0	0	0	0	0	0
X	0	0	0	0	2	0	0	0	0	0	0	0	0
Y	0	0	0	0	2	0	0	0	0	0	0	39	0

X, Y = sex chromosomes.

Table 5
RT targets of upregulated piRNAs (fold change ≥ 4, p < 0.001) in the human chromosomes.[a]

	Upregulated piRNAs in CS					Upregulated piRNAs in CDC					Upregulated piRNAs in CF		
RT	DQ570332	DQ578426	DQ579582	DQ591185	DQ592096	DQ570326	DQ570339	DQ578783	DQ582302	DQ582496	DQ579896	DQ578075	DQ581624
CR1	5	3	1	6	6	0	0	1	0	3	1	3	0
LINE-1	115	119	41	84	428	0	0	48	0	41	12	97	0
LINE-2	8	2	9	12	49	0	0	11	0	5	7	32	0

[a] All targets presented belong to the LINE class. The numbers indicate the cumulative total repeats of a RT present in 1–100,000 bases of human chromosomes.

induce the inhibition of LINE-1 expression and, consequently, activate AKT signaling (Lucchinetti et al., 2006).

3.4. piRNA deregulation is associated with L1 reduction and AKT signaling activation in cardiac progenitors

Considering the important role of the L1 inhibition and the AKT signaling activation in reducing heart damage (Lucchinetti et al., 2006), we first compared L1 mRNA level in the three cell types. Among different methods available for the analysis of L1 expression (Munoz-Lopez et al., 2012), we chose qRT-PCR. To accurately quantify L1 mRNA levels, two different sets of primers and probes were used to amplify 67- and 64-bp amplicons from the 5′-UTR and ORF2 regions of L1, respectively.

Notably as expected, and as previously demonstrated (Coufal et al., 2009), the level of L1 mRNA obtained using the ORF2 set is higher than the level obtained with the 5′-UTR set (data not shown).

As shown in Fig. 4C and D, in general, L1 transcript levels were markedly decreased in CDC and CS, in comparison to CF ($p < 0.01$), confirming the *in silico* prediction.

Next, we investigated the activation status of AKT pathway by determining the expression of phosphorylated AKT (S473) in CDC, CS and CF ($n = 3$ for each cell types). Phosphorylated AKT levels were significantly higher in CDC and CS (more than twofold) than in CF ($p < 0.01$, Fig. 4E–H).

As part of this experiment, we examined whether a representative AKT downstream signaling molecule, such as GSK3β, was also modulated. GSK3β is a kinase whose activity is inhibited by phosphorylation of Ser9 by phospho-AKT. In CDC and, especially, in CS ($p < 0.05$), the phosphorylation of AKT (Ser473) was associated with the phosphorylation of GSK3β (Ser9) (Fig. 4E and I).

These results unequivocally demonstrated that, in cardiac progenitors, the reduction of L1 expression is accompanied by a higher activation of AKT pathway.

4. Discussion

In the last decade CPC have attracted great interest as an *in vitro* model of a stem cell niche-like microenvironment (Barile et al., 2013) and as a possible source for myocardial regenerative therapies (Makkar et al., 2012). Because of their use in clinical trials, many efforts have been made to better characterize CPC, particularly focusing on the impact of age and disease on cardiac progenitors' features.

Although it has been shown that c-KIT expression, CDC proliferation and their regenerative potential declined with advancing age (Capogrossi, 2004; Mishra et al., 2011), CDC can be successfully produced from adults (Chan et al., 2012; Hsiao et al., 2013; Moretti et al., 2006) and they are functionally competent (Simpson et al., 2012), representing a promising new approach to treat patients with ischemic heart failure.

Recently, several studies highlighted the role of ncRNAs in cardiac regeneration and heart diseases (Wu et al., 2013), so that miRNA mimics and/or inhibitors have been envisaged to treat heart diseases (van Rooij and Olson, 2012). PiRNAs are small ncRNAs associated with PIWI proteins, which are expressed not only in germ but also somatic cells of various organs, including brain, liver and heart (Law et al., 2013; Rajan et al., 2014). PiRNAs are able to

modulate transposons expression (Kim, 2006) and key molecular pathways (Watanabe et al., 2006) as AKT signaling. In particular, it has been shown that abundant piRNA expression induces AKT activation (Law et al., 2013). Moreover, Rajan et al. showed as both miRNAs and piRNAs alter AKT pathway in heart diseases (Rajan et al., 2014). AKT is a powerful survival signal, and it plays a vital function in heart enhancing the proliferation of myocardial stem and progenitor cells and cardiomyocyte survival (Fujio et al., 2000; Matsui et al., 1999; Matsui et al., 2001; Rajan et al., 2014).

Remarkably, the AKT signaling pathway is activated by many cardioprotective ligand-receptor systems (Baines et al., 1999; Buerke et al., 1995; Dudek et al., 1997; Hirota et al., 1999; Kulik et al., 1997; Li et al., 1999; Oh et al., 1998). Notably, the deregulation of AKT pathway is involved in heart remodelling and decompensation, contributing to the development of heart diseases (Dent et al., 2007).

Since several evidences have shown the central role of this pathway in myocardial biology, AKT has been considered an interesting target for controlling many important aspects of myocardial biological processes and for improving cardiac repair. Despite many efforts have been done, there were several limitations in the AKT manipulation (Sussman, 2007; Sussman et al., 2011). For this reason, in-depth studies of the molecular mechanisms underlying the regulation of AKT have been necessary.

Interestingly, it was demonstrated that the AKT signaling pathway is activated by the inhibition of LINE-1, leading to a decrease of cardiac ischemic damage (Lucchinetti et al., 2006). All these evidences reveal how piRNAs are crucial players in the regulatory network governing cardiac physiology and pathology. Indeed, very recently, Rajan and coworkers showed an altered piRNA expression in an animal model of cardiac hypertrophy and identified the presence of a specific piRNA in sera of patients with myocardial infarction, suggesting a role of piRNAs in the retrotransposon mechanisms activated during several cardiac pathologies (Rajan et al., 2016).

In this scenario, our study provides a full and comprehensive list of piRNAs expressed in CPC, describing differentially expressed piRNAs within the three cell types, irrespectively of heart diseases. To our knowledge, this is the first report of piRNA signature in cardiac progenitors, suggesting a role for piRNAs in cardiac regenerative potential.

Microarray results revealed a set of differentially expressed piRNAs, with 641 upregulated and 1301 downregulated piRNAs in CS compared to CDC, while 255 and 708 piRNAs resulted up- and down-regulated, respectively, comparing CS to CF. We also identified 181 piRNAs that are overexpressed and 129 downexpressed in CDC in respect to CF.

Intriguingly, based on piRNA profiles, hierarchical clustering analysis clearly arranges samples showing systematic variations in the expression of piRNAs within the three cell types. In addition, some piRNAs were highly expressed only in one of the three cell types analysed, suggesting their role in the cell phenotype determination.

Bioinformatics analysis also showed that the deregulated piRNAs were distributed overall the genome with higher density on few chromosomes, suggesting that piRNAs are organized in discrete genomic clusters, as reported (O'Donnell and Boeke, 2007). Moreover, *in silico* prediction indicates that the most upregulated piRNAs target transposons spread among the human chromosomes, especially LINE-1. This prediction was confirmed by qRT-PCR, which highlighted a decrease of L1 transcripts in CDC and CS, in comparison to cardiac fibroblasts. The L1 reduction is also associated to an activation of AKT signaling, as shown by Western Blot analysis. These data are in line with the known piRNA-mediated reduction of LINE-1, which influences AKT signaling pathway (Lucchinetti et al., 2006; Rajan et al., 2014). However, the mechanisms integrating piRNAs with crucial molecular pathways are still poorly understood and the pathophysiological significance of piRNAs in heart is not currently known.

The present study identifies for the first time a cardiac piRNome which may be, at least partially, responsible of the different regenerative potential and may shed new lights on the understanding the complex molecular mechanisms of cardiac regeneration. Although the present study indicates a cell-type specific piRNA signature, future functional studies will be necessary in order to unravel the mechanisms in which these non-coding RNAs are involved, and to determine their role in cardiac regeneration.

Conflict of interest

The authors declare no conflict of interest.

Funding

This work was supported by Italian Ministry of University and Research (MIUR) by means of the national Program PON REC 2007–2013, projects PON 02_00607_3621894 and PON02_00607_3421644.

Acknowledgements

We thank Salvatore Pasqua, Diego Sebastian Paini and Lucia D'Aiello for skilful technical assistance.

Appendix A. Supplementary data

Supplementary data associated with this article can be found, in the online version, at http://dx.doi.org/10.1016/j.biocel.2016.04.012.

References

Ach, R.A., Wang, H., Curry, B., 2008. Measuring microRNAs: comparisons of microarray and quantitative PCR measurements, and of different total RNA prep methods. BMC Biotechnol. 8 (September), 69.
Aguirre, A., Sancho-Martinez, I., Izpisua Belmonte, J.C., 2013. Reprogramming toward heart regeneration: stem cells and beyond. Cell Stem Cell 12, 275–284.
Aguirre, A., Montserrat, N., Zacchigna, S., Nivet, E., Hishida, T., Krause, M.N., et al., 2014. In vivo activation of a conserved microRNA program induces mammalian heart regeneration. Cell Stem Cell 15, 589–604.
Aravin, A., Gaidatzis, D., Pfeffer, S., Lagos-Quintana, M., Landgraf, P., Iovino, N., et al., 2006. A novel class of small RNAs bind to MILI protein in mouse testes. Nature 442, 203–207.
Aravin, A.A., Sachidanandam, R., Girard, A., Fejes-Toth, K., Hannon, G.J., 2007. Developmentally regulated piRNA clusters implicate MILI in transposon control. Science 316, 744–747.
Baines, C.P., Wang, L., Cohen, M.V., Downey, J.M., 1999. Myocardial protection by insulin is dependent on phospatidylinositol 3-kinase but not protein kinase C or KATP channels in the isolated rabbit heart. Basic Res. Cardiol. 94, 188–198.
Barile, L., Gherghiceanu, M., Popescu, L.M., Moccetti, T., Vassalli, G., 2013. Human cardiospheres as a source of multipotent stem and progenitor cells. Stem Cells Int. 2013, 916837.
Barile, L., Lionetti, V., Cervio, E., Matteucci, M., Gherghiceanu, M., Popescu, L.M., et al., 2014. Extracellular vesicles from human cardiac progenitor cells inhibit cardiomyocyte apoptosis and improve cardiac function after myocardial infarction. Cardiovasc. Res. 103, 530–541.
Brennecke, J., Aravin, A.A., Stark, A., Dus, M., Kellis, M., Sachidanandam, R., et al., 2007. Discrete small RNA-generating loci as master regulators of transposon activity in *Drosophila*. Cell 128, 1089–1103.
Buerke, M., Murohara, T., Skurk, C., Nuss, C., Tomaselli, K., Lefer, A.M., 1995. Cardioprotective effect of insulin-like growth factor I in myocardial ischemia followed by reperfusion. Proc. Natl. Acad. Sci. U. S. A. 92, 8031–8035.
Capogrossi, M.C., 2004. Cardiac stem cells fail with aging: a new mechanism for the age-dependent decline in cardiac function. Circ. Res. 94, 411–413.
Chan, H.H., Meher Homji, Z., Gomes, R.S., Sweeney, D., Thomas, G.N., Tan, J.J., et al., 2012. Human cardiosphere-derived cells from patients with chronic ischaemic heart disease can be routinely expanded from atrial but not epicardial ventricular biopsies. J. Cardiovasc. Trans. Res. 5, 678–687.
Chimenti, I., Smith, R.R., Li, T.S., Gerstenblith, G., Messina, E., Giacomello, A., et al., 2010. Relative roles of direct regeneration versus paracrine effects of human

cardiosphere-derived cells transplanted into infarcted mice. Circ. Res. 106, 971–980.
Chimenti, I., Gaetani, R., Barile, L., Forte, E., Ionta, V., Angelini, F., et al., 2012. Isolation and expansion of adult cardiac stem/progenitor cells in the form of cardiospheres from human cardiac biopsies and murine hearts. Methods Mol. Biol. 879, 327–338.
Chuaqui, R.F., Bonner, R.F., Best, C.J., Gillespie, J.W., Flaig, M.J., Hewitt, S.M., et al., 2002. Post-analysis follow-up and validation of microarray experiments. Nat. Genet. 32 (Suppl), 509–514.
Coufal, N.G., Garcia-Perez, J.L., Peng, G.E., Yeo, G.W., Mu, Y., Lovci, M.T., et al., 2009. L1 retrotransposition in human neural progenitor cells. Nature 460, 1127–1131.
Dallas, P.B., Gottardo, N.G., Firth, M.J., Beesley, A.H., Hoffmann, K., Terry, P.A., et al., 2005. Gene expression levels assessed by oligonucleotide microarray analysis and quantitative real-time RT-PCR— how well do they correlate? BMC Genomics 6, 59.
Dent, M.R., Das, S., Dhalla, N.S., 2007. Alterations in both death and survival signals for apoptosis in heart failure due to volume overload. J. Mol. Cell. Cardiol. 43, 726–732.
Di Giacomo, M., Comazzetto, S., Saini, H., De Fazio, S., Carrieri, C., Morgan, M., et al., 2013. Multiple epigenetic mechanisms and the piRNA pathway enforce LINE1 silencing during adult spermatogenesis. Mol. Cell 50, 601–608.
Dudek, H., Datta, S.R., Franke, T.F., Birnbaum, M.J., Yao, R., Cooper, G.M., et al., 1997. Regulation of neuronal survival by the serine-threonine protein kinase Akt. Science 275, 661–665.
Eulalio, A., Mano, M., Dal Ferro, M., Zentilin, L., Sinagra, G., Zacchigna, S., et al., 2012. Functional screening identifies miRNAs inducing cardiac regeneration. Nature 492, 376–381.
Fujio, Y., Nguyen, T., Wencker, D., Kitsis, R.N., Walsh, K., 2000. Akt promotes survival of cardiomyocytes in vitro and protects against ischemia-reperfusion injury in mouse heart. Circulation 101, 660–667.
Girard, A., Sachidanandam, R., Hannon, G.J., Carmell, M.A., 2006. A germline-specific class of small RNAs binds mammalian Piwi proteins. Nature 442, 199–202.
Ha, H., Song, J., Wang, S., Kapusta, A., Feschotte, C., Chen, K.C., et al., 2014. A comprehensive analysis of piRNAs from adult human testis and their relationship with genes and mobile elements. BMC Genomics 15, 545.
Hirota, H., Chen, J., Betz, U.A., Rajewsky, K., Gu, Y., Ross Jr., J., et al., 1999. Loss of a gp130 cardiac muscle cell survival pathway is a critical event in the onset of heart failure during biomechanical stress. Cell 97, 189–198.
Hsiao, L.C., Carr, C., Chang, K.C., Lin, S.Z., Clarke, K., 2013. Stem cell-based therapy for ischemic heart disease. Cell Transplant. 22, 663–675.
Iwasaki, Y.W., Siomi, M.C., Siomi, H., 2015. PIWI-Interacting RNA: its biogenesis and functions. Annu. Rev. Biochem. 84, 405–433.
Kim, V.N., 2006. Small RNAs just got bigger: piwi-interacting RNAs (piRNAs) in mammalian testes. Genes Dev. 20, 1993–1997.
Kulik, G., Klippel, A., Weber, M.J., 1997. Antiapoptotic signalling by the insulin-like growth factor I receptor, phosphatidylinositol 3-kinase, and Akt. Mol. Cell. Biol. 17, 1595–1606.
Law, P.T., Qin, H., Ching, A.K., Lai, K.P., Co, N.N., He, M., et al., 2013. Deep sequencing of small RNA transcriptome reveals novel non-coding RNAs in hepatocellular carcinoma. J. Hepatol. 58, 1165–1173.
Lee, E.J., Banerjee, S., Zhou, H., Jammalamadaka, A., Arcila, M., Manjunath, B.S., et al., 2011. Identification of piRNAs in the central nervous system. RNA 17, 1090–1099.
Li, B., Setoguchi, M., Wang, X., Andreoli, A.M., Leri, A., Malhotra, A., et al., 1999. Insulin-like growth factor-1 attenuates the detrimental impact of nonocclusive coronary artery constriction on the heart. Circ. Res. 84, 1007–1019.
Li, T.S., Cheng, K., Lee, S.T., Matsushita, S., Davis, D., Malliaras, K., et al., 2010. Cardiospheres recapitulate a niche-like microenvironment rich in stemness and cell-matrix interactions, rationalizing their enhanced functional potency for myocardial repair. Stem Cells 28, 2088–2098.
Lin, Z., Zhou, P., von Gise, A., Gu, F., Ma, Q., Chen, J., et al., 2015. Pi3kcb links Hippo-YAP and PI3K-AKT signaling pathways to promote cardiomyocyte proliferation and survival. Circ. Res. 116, 35–45.
Lucchinetti, E., Feng, J., Silva, R., Tolstonog, G.V., Schaub, M.C., Schumann, G.G., et al., 2006. Inhibition of LINE-1 expression in the heart decreases ischemic damage by activation of Akt/PKB signaling. Physiol. Genomics 25, 314–324.
Makkar, R.R., Smith, R.R., Cheng, K., Malliaras, K., Thomson, L.E., Berman, D., et al., 2012. Intracoronary cardiosphere-derived cells for heart regeneration after myocardial infarction (CADUCEUS): a prospective, randomised phase 1 trial. Lancet 379, 895–904.
Mathieu, J., Ruohola-Baker, H., 2013. Regulation of stem cell populations by microRNAs. Adv. Exp. Med. Biol. 786, 329–351.
Matsui, T., Li, L., del Monte, F., Fukui, Y., Franke, T.F., Hajjar, R.J., et al., 1999. Adenoviral gene transfer of activated phosphatidylinositol 3'-kinase and Akt inhibits apoptosis of hypoxic cardiomyocytes in vitro. Circulation 100, 2373–2379.
Matsui, T., Tao, J., del Monte, F., Lee, K.H., Li, L., Picard, M., et al., 2001. Akt activation preserves cardiac function and prevents injury after transient cardiac ischemia in vivo. Circulation 104, 330–335.
Messina, E., De Angelis, L., Frati, G., Morrone, S., Chimenti, S., Fiordaliso, F., et al., 2004. Isolation and expansion of adult cardiac stem cells from human and murine heart. Circ. Res. 95, 911–921.
Mishra, R., Vijayan, K., Colletti, E.J., Harrington, D.A., Matthiesen, T.S., Simpson, D., et al., 2011. Characterization and functionality of cardiac progenitor cells in congenital heart patients. Circulation 123, 364–373.
Moretti, A., Caron, L., Nakano, A., Lam, J.T., Bernshausen, A., Chen, Y., et al., 2006. Multipotent embryonic isl1+ progenitor cells lead to cardiac, smooth muscle, and endothelial cell diversification. Cell 127, 1151–1165.
Morey, J.S., Ryan, J.C., Van Dolah, F.M., 2006. Microarray validation: factors influencing correlation between oligonucleotide microarrays and real-time PCR. Biol. Proced. Online 8, 175–193.
Moyano, M., Stefani, G., 2015. piRNA involvement in genome stability and human cancer. J. Hematol. Oncol. 8, 38.
Munoz-Lopez, M., Garcia-Canadas, M., Macia, A., Morell, S., Garcia-Perez, J.L., 2012. Analysis of LINE-1 expression in human pluripotent cells. Methods Mol. Biol. 873, 113–125.
Nichols, M., Townsend, N., Scarborough, P., Rayner, M., 2014. Cardiovascular disease in Europe epidemiological update. Eur. Heart J. 35, 2929.
O'Donnell, K.A., Boeke, J.D., 2007. Mighty Piwis defend the germline against genome intruders. Cell 129, 37–44.
Oh, H., Fujio, Y., Kunisada, K., Hirota, H., Matsui, H., Kishimoto, T., et al., 1998. Activation of phosphatidylinositol 3-kinase through glycoprotein 130 induces protein kinase B and p70 S6 kinase phosphorylation in cardiac myocytes. J. Biol. Chem. 273, 9703–9710.
Olson, E.N., 2014. MicroRNAs as therapeutic targets and biomarkers of cardiovascular disease. Sci. Transl. Med. 6, 239ps3.
Ounzain, S., Crippa, S., Pedrazzini, T., 2013. Small and long non-coding RNAs in cardiac homeostasis and regeneration. Biochim. Biophys. Acta 1833, 923–933.
Philippen, L.E., Dirkx, E., da Costa-Martins, P.A., De Windt, L.J., 2015. Non-coding RNA in control of gene regulatory programs in cardiac development and disease. J. Mol. Cell. Cardiol. 89 (Pt A), 51–58.
Pisano, F., Altomare, C., Cervio, E., Barile, L., Rocchetti, M., Ciuffreda, M.C., et al., 2015. Combination of miRNA499 and miRNA133 exerts a synergic effect on cardiac differentiation. Stem Cells 33, 1187–1199.
Rajan, K.S., Velmurugan, G., Pandi, G., 2014. Ramasamy S: miRNA and piRNA mediated Akt pathway in heart: antisense expands to survive. Int. J. Biochem. Cell Biol. 55, 153–156.
Rajan, K.S., Velmurugan, G., Gopal, P., Ramprasath, T., Babu, D.D., Krithika, S., et al., 2016. Abundant and altered expression of PIWI-Interacting RNAs during cardiac hypertrophy. Heart Lung Circ., http://dx.doi.org/10.1016/j.hlc.2016.02.015, pii: S1443-9506(16)30034-8.
Samji, T., 2009. PIWI, piRNAs, and germline stem cells: what's the link. Yale J. Biol. Med. 82, 121–124.
Seto, A.G., Kingston, R.E., Lau, N.C., 2007. The coming of age for Piwi proteins. Mol. Cell 26, 603–609.
Sharma, A.K., Nelson, M.C., Brandt, J.E., Wessman, M., Mahmud, N., Weller, K.P., et al., 2001. Human CD34(+) stem cells express the hiwi gene, a human homologue of the *Drosophila* gene piwi. Blood 97, 426–434.
Simpson, D.L., Mishra, R., Sharma, S., Goh, S.K., Deshmukh, S., Kaushal, S., 2012. A strong regenerative ability of cardiac stem cells derived from neonatal hearts. Circulation 126, S46–53.
Siomi, M.C., Sato, K., Pezic, D., Aravin, A.A., 2011. PIWI-interacting small RNAs: the vanguard of genome defence. Nat. Rev. Mol. Cell Biol. 12, 246–258.
Smith, R.R., Barile, L., Cho, H.C., Leppo, M.K., Hare, J.M., Messina, E., et al., 2007. Regenerative potential of cardiosphere-derived cells expanded from percutaneous endomyocardial biopsy specimens. Circulation 115, 896–908.
Sussman, M.A., Volkers, M., Fischer, K., Bailey, B., Cottage, C.T., Din, S., et al., 2011. Myocardial AKT: the omnipresent nexus. Physiol. Rev. 91, 1023–1070.
Sussman, M., 2007. AKTing lessons for stem cells: regulation of cardiac myocyte and progenitor cell proliferation. Trends Cardiovasc. Med. 17, 235–240.
Watanabe, T., Takeda, A., Tsukiyama, T., Mise, K., Okuno, T., Sasaki, H., et al., 2006. Identification and characterization of two novel classes of small RNAs in the mouse germline: retrotransposon-derived siRNAs in oocytes and germline small RNAs in testes. Genes Dev. 20, 1732–1743.
Weick, E.M., Miska, E.A., 2014. piRNAs: from biogenesis to function. Development 141, 3458–3471.
Wu, S.M., Chien, K.R., Mummery, C., 2008. Origins and fates of cardiovascular progenitor cells. Cell 132, 537–543.
Wu, G., Huang, Z.P., Wang, D.Z., 2013. MicroRNAs in cardiac regeneration and cardiovascular disease. Sci. China Life Sci. 56, 907–913.
Yeh, R.W., Sidney, S., Chandra, M., Sorel, M., Selby, J.V., Go, A.S., 2010. Population trends in the incidence and outcomes of acute myocardial infarction. N. Engl. J. Med. 362, 2155–2165.
Yuen, T., Wurmbach, E., Pfeffer, R.L., Ebersole, B.J., Sealfon, S.C., 2002. Accuracy and calibration of commercial oligonucleotide and custom cDNA microarrays. Nucleic Acids Res. 30, e48.
van Rooij, E., Olson, E.N., 2012. MicroRNA therapeutics for cardiovascular disease: opportunities and obstacles. Nat. Rev. Drug Discov. 11, 860–872.
Zhang, Y., Mignone, J., MacLellan, W.R., 2015. Cardiac regeneration and stem cells. Physiol. Rev. 95, 1189–1204.